

Article

Acidic Stabilization of the Dual-Aromatic Heterocyclic Anions

Chongyang Li^{1,2}, Yongli Huang^{1,*}, Chang Q Sun^{3,4} and Lei Zhang^{2,5,*} 

¹ Key Laboratory of Low-Dimensional Materials and Application Technology (Ministry of Education), School of Materials Science and Engineering, Xiangtan University, Xiangtan 411105, China; lichongyang199310@163.com

² CAEP Software Center for High Performance Numerical Simulation, Beijing 100088, China

³ EBEAM, Yangtze Normal University, Chongqing 408100, China; ecqsun@gmail.com

⁴ NOVITAS, Nanyang Technological University, Singapore 639798, Singapore

⁵ Institute of Applied Physics and Computational Mathematics, Beijing 100088, China

* Correspondence: huangyongli@xtu.edu.cn (Y.H.); zhang_lei@iapcm.ac.cn (L.Z.)

Abstract: Recently, we discovered that the delocalization of nitrogen lone-pair electrons (NLPEs) in five-membered nitrogen heterocycles created a second σ -aromaticity in addition to the prototypical π -aromaticity. Such dual-aromatic compounds, such as the pentazole anion, were proved to have distinct chemistry in comparison to traditional π -aromatics, such as benzene, and were surprisingly unstable, susceptible to electrophilic attack, and relatively difficult to obtain. The dual-aromatics are basic in nature, but prefer not to be protonated when confronting more than three hydronium/ammonium ions, which violates common sense understanding of acid–base neutralization for a reason that is unclear. Here, we carried out 63 test simulations to explore the stability and reactivity of three basic heterocycle anions (pentazole anion N_5^- , tetrazole anion $N_4C_1H_1^-$, and 1,2,4-triazole anion $N_3C_2H_2^-$) in four types of solvents (acidic ions, H_3O^+ and NH_4^+ , polar organics, THF, and neutral organics, benzene) with different acidities and concentrations. By quantum mechanical calculations of the electron density, atomistic structure, interatomic interactions, molecular orbital, magnetic shielding, and energetics, we confirmed the presence of dual aromaticity in the heterocyclic anions, and discovered their reactivity to be a competition between their basicity and dual aromaticity. Interestingly, when the acidic ions H_3O^+/NH_4^+ are three times more in number than the basic heterocyclic anions, the anions turn to violate acid–base neutralization and remain unprotonated, and the surrounding acidic ions start to show a significant stabilization effect on the studied heterocyclic anions. This work brings new knowledge to nitrogen aromatics and the finding is expected to be adaptable for other pnictogen five-membered ring systems.

Keywords: acidic stabilization; dual-aromaticity; heterocyclic anions; quantum mechanics calculations



Citation: Li, C.; Huang, Y.; Sun, C.Q.; Zhang, L. Acidic Stabilization of the Dual-Aromatic Heterocyclic Anions. *Catalysts* **2021**, *11*, 766. <https://doi.org/10.3390/catal11070766>

Academic Editor: Gianluigi Albano

Received: 6 June 2021

Accepted: 21 June 2021

Published: 24 June 2021

Publisher's Note: MDPI stays neutral with regard to jurisdictional claims in published maps and institutional affiliations.



Copyright: © 2021 by the authors. Licensee MDPI, Basel, Switzerland. This article is an open access article distributed under the terms and conditions of the Creative Commons Attribution (CC BY) license (<https://creativecommons.org/licenses/by/4.0/>).

1. Introduction

Nitrogen-rich, high-energy-density materials (HEDMs), in which the nitrogen weight is higher than 50% [1], are known to generate a large amount of heat when exothermically decomposing into molecular dinitrogen [2]. In addition, a considerable amount of nitrogen-rich HEDMs also show low-shock sensitivity, improved burning rate, and other advanced advantages [3]. Therefore, nitrogen-rich HEDMs are very promising candidates to address the long-standing, high-energy density and low-sensitivity contradiction of HEDMs, and can potentially be utilized to safely conduct space exploration, explore ultra-deep mineral deposits on Earth, and so forth [4–9]. For example, 3-nitro-1,2,4-triazole-5-one (NTO) has a high-energy density (comparable to RDX) and low sensitivity (lower than HMX), and has become a very important ingredient in the polymer-bonded explosive (PBX) formulations for insensitive munitions (IMs) [1,10,11]. Triaminoguanidinium azotetrazolate (TAGzT) can increase the heat generation and burning rates of propellants over a wide pressure range [3]. 5,5'-hydrazinebistetrazole (HBT) and bis (3,4,5-triamino-1,2,4-triazolium) 5,5'-azotetrazolate (G₂ZT) contain up to ~80% of nitrogen weight and present a relatively high

combustion heat (-2396 cal/g for HBT and -2775 cal/g for G₂ZT) [12]. In particular, the pentazole anion has a nitrogen weight of 100% and its reaction product consists only of molecular dinitrogen. Therefore, the pentazole anion is considered the ultimate in the pursuit of energetic material that is green, non-polluting, and ultra-high energetic [1].

Due to the above satisfactory comprehensive properties, nitrogen-rich HEDMs, such as triazoles, tetrazoles, and pentazoles, are extensively used as building blocks for the design of advanced, new HEDMs [1,13–21]. However, the stabilization mechanism of nitrogen heterocycles, which is essential for the rational design and large-scale production of advanced HEDMs, remains unclear. The problem is mainly focused on the distributions and states of the nitrogen lone-pair electrons (NLPEs), and their influence on the structural stability and chemical reactivity of heterocycles. For example, the valence shell electron pair repulsion (VSEPR) theory suggests that the NLPEs are localized in the vicinity of each separate nitrogen atom. Therefore, the NLPEs in a cyclic system should repel the adjacent C–N bonds and other lone pairs in the ring [22–24], thereby destabilizing the system. However, this derivation contradicts the fact that the presence of nitrogen in the ring can actually impart a higher degree of stability to these molecules compared to their hydrocarbon analogs [22,25]. To interpret this “aza-stabilization” anomaly, some researchers have proposed that the NLPEs are delocalized over the cyclic systems instead of being localized on separate nitrogen atoms [25,26]. However, this proposition is again challenged by the elusive chemistry of the pentazole anion. The pentazole anion has five nitrogen atoms and one π -electron aromatic system and, theoretically, it should be very stable. However, the pentazole anion has been proved to be surprisingly unstable, difficult to obtain, and susceptible to electrophilic attack [26–32]. The pentazole anion is basic in nature, but prefers not to be protonated when facing more than three hydronium/ammonium ions [28,33], which violates the acid–base neutralization rule for reasons that are unclear. Therefore, a better understanding of the stabilization and reactivity of nitrogen heterocyclic species requires new knowledge of nitrogen chemistry.

Recently, we discovered that the delocalization of NLPEs in five-membered nitrogen heterocycles creates a second σ -aromaticity, in addition to the prototypical π -aromaticity [34,35]. Taking the pentazole anion as an example, it has five nitrogen atoms in a planar ring and all the nitrogen atoms are sp^2 hybridized. Six electrons at the $2p_z$ π molecular orbital (MO) constitute a complete π aromatic system, and ten NLPEs at the $2sp^2$ σ MO give rise to an additional σ aromatic system. The dual-aromatic system features a simultaneous delocalization of the π electrons above/below the plane and the σ lone-pair electrons in the equatorial plane, which is very different from the multi-aromaticity of all-metal systems caused by an electron deficiency. Such dual-aromatic heterocyclic compounds were proved to have distinct chemistry in comparison to traditional π -aromatics, such as benzene. In vacuums, solutions, and crystals, the pentazole anion is protonated when facing less than three H_3O^+/NH_4^+ ions, and prefers not to be protonated when the number of H_3O^+/NH_4^+ ions is more than three. It is the compatible coexistence of the inter-lone-pair repulsion and inter-lone-pair attraction within the σ -aromatic system that makes the stability and reactivity of these dual-aromatics vary according to their environments [34].

In this work, we designed and conducted a series of quantum mechanical calculations to explore the structural stability and chemical reactivity of three heterocyclic anions in four types of solvents with different acidity and concentrations. Interestingly, when the acidic H_3O^+/NH_4^+ ions are three times more in number than the heterocyclic anions, they start to show a stabilization effect on the structural stability of the studied heterocycles. The detailed calculation results and proposed mechanism are shown below.

2. Results and Discussion

2.1. Presence of Dual Aromaticity in the Heterocyclic Anions Studied

From the atomic orbital diagrams in Figure 1, all the carbon and nitrogen atoms in N_5^- , $N_4C_1H_1^-$, and $N_3C_2H_2^-$ were sp^2 hybridized. Taking into account the net foreign electron, which resided at the p orbital, each of the three heterocyclic anions obtained six π electrons,

respectively, forming a complete π -aromatic system. The isosurface of the lowest π MO ($\text{MO}_{\text{min-}\pi}$) presented a shape spreading out over the entire molecule above and below each molecular plane. The delocalization index $\text{DI}_{\text{min-}\pi}$ was calculated to be 0.16 between any two atoms (nearest neighbors and second nearest neighbors) in the ring, thus confirming the full delocalization of the electrons at this minimum π orbital. As shown at the bottom of Figure 1, $\text{NICS}_{\text{zz}}(r)_\pi$ was always negative when the vertical distance relative to each ring critical point (r) varied from 0.0 to 5.0 Å, thereby confirming the presence of π -aromaticity in the three heterocyclic anions. By comparing the calculated $\text{NICS}_{\text{zz}}(1)_\pi$ of the three anions, the order of their π -aromaticity was $\text{N}_5^- (-26.1) > \text{N}_4\text{C}_1\text{H}_1^- (-25.8) > \text{N}_3\text{C}_2\text{H}_2^- (-25.2)$. Compared with benzene, which had $\text{DI}_{\text{min-}\pi} = 0.11$ and $\text{NICS}_{\text{zz}}(1)_\pi = -28.96$, the three heterocyclic anions presented a higher level of electron delocalization, but a weaker π -aromaticity.

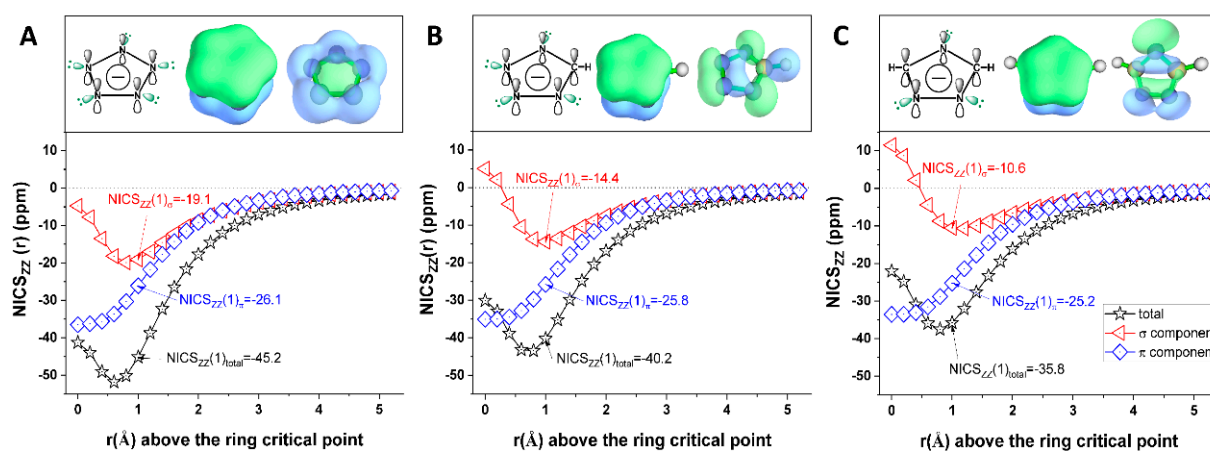


Figure 1. Confirmation of presence of dual aromaticity in (A) pentazole anion N_5^- , (B) tetrazole anion $\text{N}_4\text{C}_1\text{H}_1^-$, and (C) 1,2,4-triazole anion $\text{N}_3\text{C}_2\text{H}_2^-$. For each anion, illustrated from top left to bottom right, are the atomic orbital diagram, top view of isosurface (0.05) of the lowest π MO ($\text{MO}_{\text{min-}\pi}$), side view of isosurface (0.05) of the lowest σ MO containing nitrogen lone pairs ($\text{MO}_{\text{min-}\sigma(\text{LP})}$), and $\text{NICS}_{\text{zz}}(r)$ (total value and its σ and π orbital components) as a function of the vertical distance relative to each ring critical point.

We next turned to the NLPE in the three heterocyclic anions. As shown by the isosurface of $\text{MO}_{\text{min-}\sigma(\text{LP})}$ at the top of Figure 1, the NLPE presented an obvious delocalization over the rings of N_5^- , $\text{N}_4\text{C}_1\text{H}_1^-$, and $\text{N}_3\text{C}_2\text{H}_2^-$, and the delocalization region expanded when more nitrogen atoms were present in the ring. Interestingly, the delocalization of the NLPE spreads out over the interior and exterior of the ring (Figure S4 of the Supplementary Materials). In $\text{N}_4\text{C}_1\text{H}_1^-$ and $\text{N}_3\text{C}_2\text{H}_2^-$, the presence of the CH bonds destroys the NLPE delocalization in the exterior of the ring, but their delocalization in the interior of the ring is not much influenced. In N_5^- , the NLPE delocalization fulfills both the interior and exterior of the ring. Correspondingly, the $\text{DI}_{\text{min-}\sigma(\text{LP})}$ values of N_5^- , $\text{N}_4\text{C}_1\text{H}_1^-$, and $\text{N}_3\text{C}_2\text{H}_2^-$ were all calculated to be 0.16, thereby confirming the NLPE delocalization at each minimum σ orbital. As shown at the bottom of Figure 1, the highest absolute value of the $\text{NICS}_{\text{zz}}(r)_\sigma$ of N_5^- was $r_{\text{extreme}} = 0.6$ Å vertically above the ring critical point, which is the same as the P_2N_3^- anion [27]; for $\text{N}_4\text{C}_1\text{H}_1^-$, $r_{\text{extreme}} = 0.8$ Å; for $\text{N}_3\text{C}_2\text{H}_2^-$, r_{extreme} shifted to 1.0 Å. As shown in Table 1, the values of $\text{NICS}_{\text{zz}}(1)_\sigma$ and $\text{NICS}_{\text{zz}}(r_{\text{extreme}})_\sigma$ were both negative, indicating the presence of an additional σ -aromaticity in the three heterocyclic anions; the order of their σ -aromaticity was $\text{N}_5^- > \text{N}_4\text{C}_1\text{H}_1^- > \text{N}_3\text{C}_2\text{H}_2^-$. The contributions of the NLPE delocalization to σ -aromaticity was also discovered in the $(\text{NH})_n$ ($n = 3-6$) systems [36].

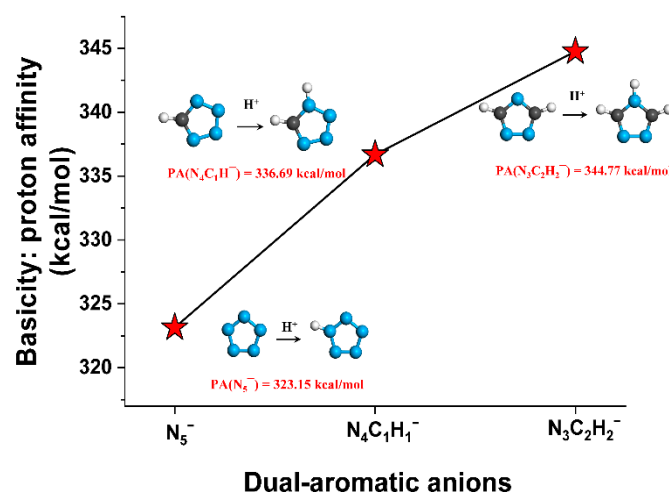
Table 1. Magnetic index of aromaticity and electron delocalization index of N_5^- , $N_4C_1H_1^-$ and $N_3C_2H_2^-$ [37].

	Indices	N_5^-	$N_4C_1H_1^-$	$N_3C_2H_2^-$	Benzene
Total	$NICS_{zz}(1)_{total}$	-45.16	-40.24	-35.78	-29.07
	$NICS_{zz}(r_{extreme})_{total}$	-51.81	-43.44	-37.53	-
π	$DI_{min-\pi}$	0.16	0.16	0.16	0.11
	$NICS_{zz}(1)_{\pi}$	-26.09	-25.81	-25.23	-28.96
σ	$DI_{min-\sigma}(LP)$	0.16	0.16	0.16	-
	$NICS_{zz}(1)_{\sigma}$	-19.06	-14.42	-10.55	-0.11
	$NICS_{zz}(r_{extreme})_{\sigma}$	-19.87	-14.42	-10.55	-

We next evaluated the total aromaticity of the three heterocyclic anions and compared them with the prototypical benzene. As shown in Table 1, the $NICS_{zz}(1)_{total}$ and $NICS_{zz}(r_{extreme})_{total}$ values both showed the order of $N_5^- > N_4C_1H_1^- > N_3C_2H_2^-$, and all three heterocyclic anions presented a stronger aromaticity than benzene. Therefore, as more nitrogen atoms are present in the heterocycles, the NLPE are more delocalized, and the σ -aromaticity and overall aromaticity increases.

2.2. Basicity of Heterocyclic Anions and Acidity of Solvents Studied

The *PA* defined by Equation (1) was employed to evaluate the basicity of the nitrogen heterocyclic anions studied; a higher *PA* corresponds to a stronger basicity. As shown in Figure 2, the value of the *PA* increased with the decrease in nitrogen atoms in the heterocyclic anion. Therefore, the sequence of their basicity was $N_5^- < N_4C_1H_1^- < N_3C_2H_2^-$, which is consistent with the order obtained from experimental pH tests ($pK_b = 9.1$ for $N_4C_1H_1^-$ and $pK_b = 4.0$ for $N_3C_2H_2^-$) [28,38].

**Figure 2.** Basicity: proton affinity of pentazole anion N_5^- , tetrazole anion $N_4C_1H_1^-$, and 1,2,4-triazole anion $N_3C_2H_2^-$.

When the *PA* is used to characterize the acidity of the solvents, a higher *PA* corresponds to a weaker acidity. As shown in Table 2, the calculated values of the *PA* were 176.3 kcal/mol for H_3O^+ , 211.9 kcal/mol for NH_4^+ , 409.7 kcal/mol for THF, and 411.1 kcal/mol for benzene, respectively. Our results were very close to the experimental results of $PA(H_3O^+) = 165.0$ kcal/mol and $PA(NH_4^+) = 204.0$ kcal/mol [39]. We also conducted a *PA* calculation for H_2O for further verification. $PA(H_2O)$ was calculated to be 396.1 kcal/mol, which was close to the experimental result of 390.3 kcal/mol [39]. The $PA(H_2O)$ value was between $PA(NH_4^+)$ and $PA(benzene)$, which was consistent with the experimental pK_a : 9.3 (NH_4^+) < 15.74 (H_2O) < 43 (benzene). From the above calculations and for verification, the order of the acidity of the solvents was $H_3O^+ > NH_4^+ > H_2O >$

benzene > THF, which was consistent with the pK_a sequence obtained from the experiments: -1.74 (H_3O^+) < 9.3 (NH_4^+) < 43 (benzene) [40].

Table 2. Basicity of heterocyclic anions and acidity of solvents studied.

Type	Compounds	PA (kcal/mol)		–Log of Dissociation Constant
		This Work	Exp.	Exp.
Heterocyclic anions	N_5^-	323.2	-	-
	$\text{N}_4\text{C}_1\text{H}_1^-$	336.7	-	$pK_b = 9.1$
	$\text{N}_3\text{C}_2\text{H}_2^-$	344.8	-	$pK_b = 4.0$
Solvents	H_3O^+	176.3	165.0 [39]	$pK_a = -1.74$ [40]
	NH_4^+	211.9	204.0 [39]	$pK_a = 9.3$ [40]
	Benzene	409.7	-	$pK_a = 43$ [40]
	THF	411.1	-	-
	H_2O	396.1	390.3 [39]	$pK_a = 15.74$ [40]

2.3. Different Reactivity of Heterocyclic Anions Depending on Solvent Types and Concentrations

Taking the solvent NH_4^+ as an example, Figure 3A presents the optimized structures of the $\text{N}_3\text{C}_2\text{H}_2^- \cdots c\text{NH}_4^+$, $\text{N}_4\text{C}_1\text{H}_1^- \cdots c\text{NH}_4^+$, and $\text{N}_5^- \cdots c\text{NH}_4^+$ complexes. When $c < 3$, the NH_4^+ ions turned to be neutral NH_3 molecules after the reaction, and the heterocyclic anions were protonated. That is, acid and base underwent a neutralization process. Correspondingly, the BE values of the three heterocyclic complexes all increased to the maximum when the NH_4^+ concentration increased from $c = 1$ to $c = 2$, as shown in Figure 3B–D. However, when $c \geq 3$, the proton would stay near NH_4^+ , and the heterocyclic anions tended to remain unprotonated, as shown by the interaction strengths (distances) of the proton with the heterocyclic anion and with solvent species in Figures S5 and S6 of the Supplementary Materials. Namely, acid and base would not proceed neutralization. Besides, the BE value of the complex started to decrease with a further increase in c , as shown in Figure 3B–D.

The effect of the H_3O^+ concentration on the reactivity of the three heterocyclic anions was similar to that of NH_4^+ , as shown in Figure S1 of the Supplementary Materials. However, the interactions between H_3O^+ and the heterocyclic anion were about 60% stronger than those between NH_4^+ and the heterocyclic anion. This resulted in $\text{H}_3\text{O}^+ \cdots$ heterocyclic complexes having higher BE values than the $\text{NH}_4^+ \cdots$ heterocyclic complexes by 28–79 kcal/mol. In benzene and THF solvents, when c varied from 1 to 5, the three heterocyclic anions were never protonated, as shown in Figures S2, S3, S5, and S6 of the Supplementary Materials. The interactions between benzene/THF and the heterocyclic anion were weak hydrogen bonds (HB, <10 kcal/mol), much weaker than the HB connected to H_3O^+ or NH_4^+ , as shown in Figure S7 of the Supplementary Materials. Correspondingly, the BE values of the benzene/THF \cdots heterocyclic complexes increased monotonously with the increase in c , but were much lower than the BE values of the $\text{H}_3\text{O}^+/\text{NH}_4^+ \cdots$ heterocyclic complexes, as shown in Figure 3B–D.

The anomaly of the reactivity of the three heterocyclic anions is that they are basic, but they prefer to be unprotonated when encountering more than three H_3O^+ or NH_4^+ ions. This not only violates the common sense of acid–base neutralization, but also leads to an increase in the total energy of the complex, as shown in Figure 3B–D. This increase in energy is caused by the mutual repulsion between the adjacent $\text{H}_3\text{O}^+/\text{NH}_4^+$, because when $c \geq 3$, the proton was in the vicinity of $\text{H}_3\text{O}^+/\text{NH}_4^+$ instead of near the heterocyclic anions. It is interesting that these $\text{H}_3\text{O}^+/\text{NH}_4^+$ ions would rather suffer mutual repulsion than diffuse away from the heterocyclic anion center. Although the protonation of N_5^- , $\text{N}_4\text{C}_1\text{H}_1^-$, and $\text{N}_3\text{C}_2\text{H}_2^-$ could eliminate this mutual electrostatic repulsion and convert intermolecular HBs into much lower energy H–N bonds to reduce the total energy of the

complex, this process did not proceed as expected when $c \geq 3$. There must be some unseen incentives to drive mutations in the reactivity of heterocyclic anions.

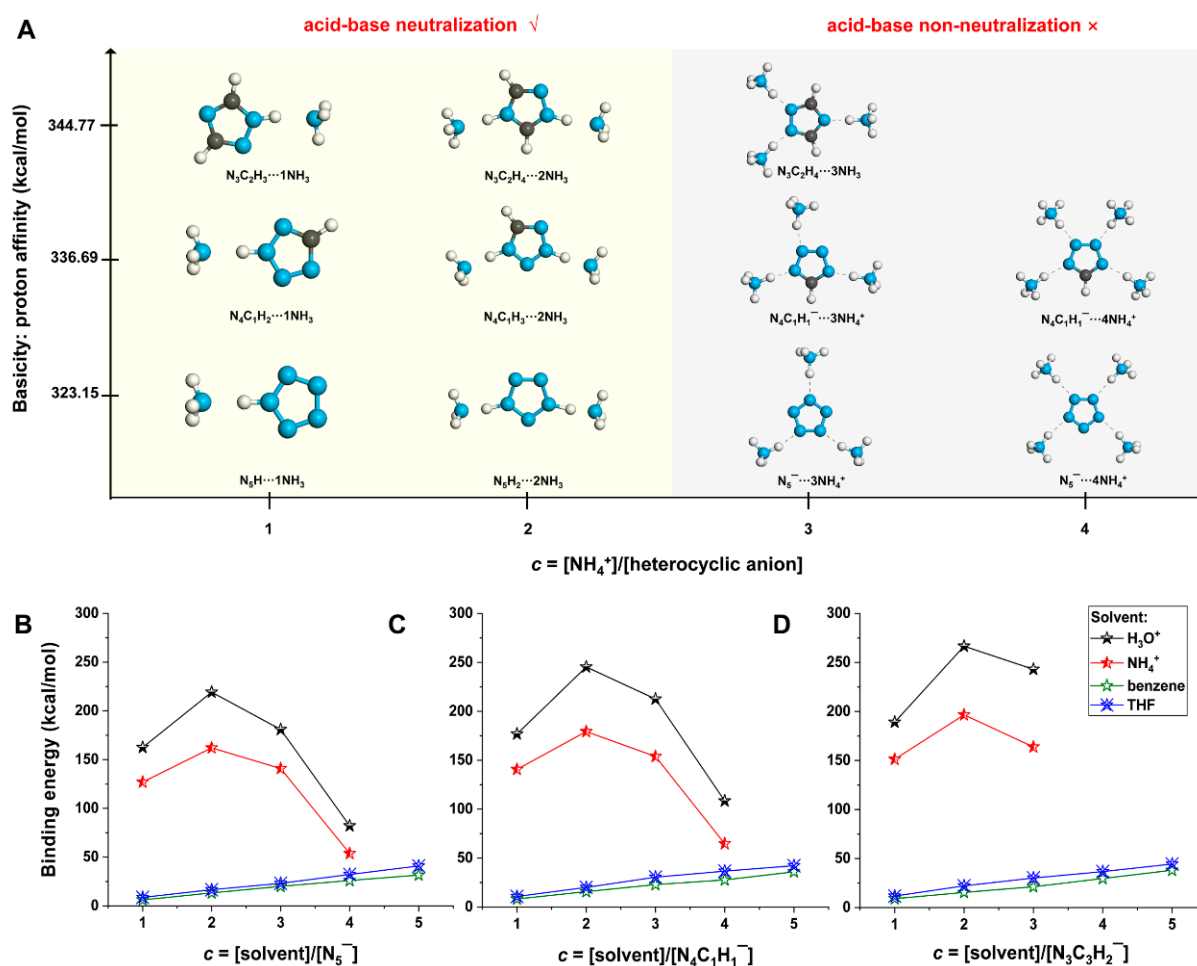


Figure 3. (A) Reactivity of $N_3C_2H_2^-$, $N_4C_1H_1^-$, and N_5^- with increasing concentration of NH_4^+ , and binding energy of (B) N_5^- complexes, (C) $N_4C_1H_1^-$ complexes, and (D) $N_3C_2H_2^-$ complexes with increasing concentration of H_3O^+ (black line), NH_4^+ (red line), benzene (olive line), and THF (blue line).

2.4. Mechanism of Anomalous Reactivity of Heterocyclic Anions

In the following, we take $N_4C_1H_1^-$ in an NH_4^+ solvent as an example to explore the mechanism of its anomalous reactivity. When $N_4C_1H_1^-$ was protonated at $c = 1$ and $c = 2$, compared with its naked state, the $DI_{\min-\sigma(LP)}$ in the ring was reduced by 0.08, and the values of $NICS_{ZZ}(1)_{total}$, $NICS_{ZZ}(1)_{\pi}$, and $NICS_{ZZ}(1)_{\sigma}$ were reduced by 2.72, 1.17, and 1.55 ppm, respectively, as shown by the red curves in Figure 4C,D and Figure S8 of the Supplementary Materials. This implied that the formation of additional single bonds consumed the delocalization of electrons in the heterocycles, thereby reducing their dual aromaticity, whereas the formation of H–N bonds could substantially lower the total energy of the complex, as shown in Figure 3A. Therefore, the basicity of $N_4C_1H_1^-$ dominated the reactivity, and the anion underwent an additional reaction by sacrificing the dual aromaticity.

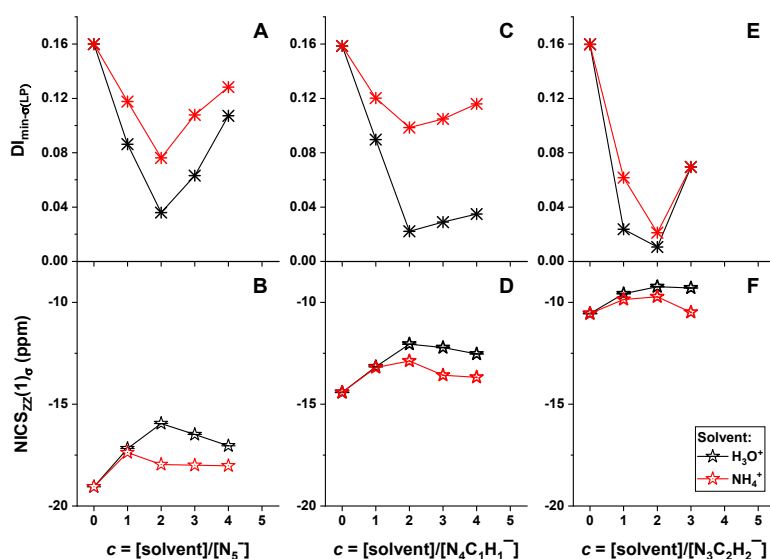


Figure 4. $DI_{\min-\sigma(LP)}$ and $NICS_{zz(1)\sigma}$ of (A,B) N_5^- , (C,D) $N_4C_1H_1^-$, and (E,F) $N_3C_2H_2^-$ with increasing concentration of H_3O^+ and NH_4^+ .

If $N_4C_1H_1^-$ continued to be protonated by more NH_4^+ , the dual aromaticity would be further weakened, which provoked $N_4C_1H_1^-$ to balance the dual aromaticity and its basicity in another way when $c \geq 3$. In order to keep the dual aromaticity intact, $N_4C_1H_1^-$ started to reduce the bonding states of electrons with nearby protons, tending to remain unprotonated and interact with all NH_4^+ through intermolecular HB. In this way, the electron delocalization of HB helped increase the dual aromaticity of $N_4C_1H_1^-$ [41]. Compared with its protonation state, the $DI_{\min-\sigma(LP)}$ in the $N_4C_1H_1^- \cdots 3NH_4^+$ complex increased by 0.03, and the aromaticity indices $NICS_{zz(1)_{total}}$, $NICS_{zz(1)\pi}$, and $NICS_{zz(1)\sigma}$ increased by 1.01, 0.31, and 0.71, respectively, as shown in Figure 4C,D. Note that at $c = 3$, the interactions of the proton with $N_4C_1H_1^-$ and NH_3 were in a critical state of competition, and σ -aromaticity is apparently the lead in changing the reactivity of $N_4C_1H_1^-$.

When $c = 4$, $N_4C_1H_1^-$ interacted with the surrounding NH_4^+ ions via typical intermolecular HBs, the $DI_{\min-\sigma(LP)}$ in the $N_4C_1H_1^- \cdots 4NH_4^+$ complex further increased by 0.03, and the aromaticity indices $NICS_{zz(1)_{total}}$, $NICS_{zz(1)\pi}$, and $NICS_{zz(1)\sigma}$ continued to increase by 0.55, 0.45, and 0.10, respectively, as shown in Figure 4C,D. That is, at $c = 4$, the dual aromaticity of $N_4C_1H_1^-$ totally defeated its basicity and totally dominated the $N_4C_1H_1^-$ to violate the acid–base neutralization.

The reaction mechanism of $N_4C_1H_1^-$ in H_3O^+ was similar to that in NH_4^+ . Because H_3O^+ ($pK_a = -1.74$ [39]) has a higher acidity than NH_4^+ ($pK_a = 9.3$ [39]), the electron delocalization and aromaticity in $N_4C_1H_1^- \cdots cH_3O^+$ presented larger variations than that in $N_4C_1H_1^- \cdots cNH_4^+$ with the increase in c , as shown in Figure 4C,D.

The proposed mechanism of the anomalous reactivity of $N_4C_1H_1^-$ is also applicable to N_5^- and $N_3C_2H_2^-$, as shown in Figure 3A. It is worth mentioning that $N_3C_2H_2^-$ contains two hydrogen atoms, repelling nearby H_3O^+/NH_4^+ ions. Therefore, this anion could have up to three H_3O^+/NH_4^+ ions in its vicinity, and the fourth H_3O^+/NH_4^+ ion was not allowed to approach thermodynamically.

2.5. Acidic Stabilization of the Dual-Aromatics Studied

It is of interest to take advantage of the discovered anomalous reactivity to catalyze a generating rate and improve the production yield of heterocycles. Taking N_5^- as an example, a successful preparation of N_5^- from the solution is to keep all the N–N bonds intact before the rupture of the C–N bond in 3,5-dimethyl-4-hydroxyphenylpentazole (HPP). Although the synthesis of N_5^- was successfully achieved with the aid of *m*-chloroperbenzoic

acid (m-CPBA) and ferrous bisglycinate [Fe(Gly)₂] [42], the production yield as well as the generating rate of N₅[−] is still to be improved and accelerated.

One of the most important preconditions of the catalysis of these heterocyclic anions is to keep their structure stable in the preparation solution. Because the strength of the C–N and N–N bonds of a heterocycle is one of the most important factors for its structural stability, we calculated all the bond strengths in the rings of N₅[−], N₄C₁H₁[−], and N₃C₂H₂[−] under different solvent concentrations. For all three heterocycles in each solvent, the weakest bonds were all N–N bonds, and their strengths were plotted as a function of *c*, as shown in Figure 5 and Figure S9 of the Supplementary Materials. The calculation method of the bond strength is detailed in the Methodology Section.

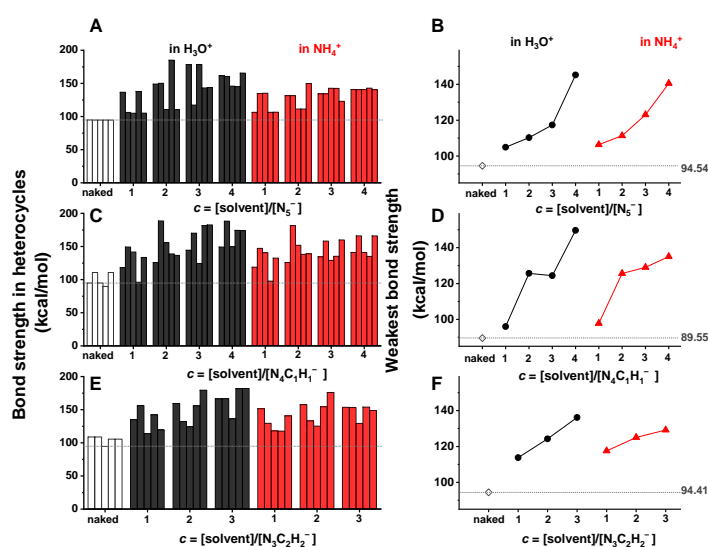


Figure 5. All bond strengths and weakest bond strengths in the rings of (A,B) N₅[−], (C,D) N₄C₁H₁[−], and (E,F) N₃C₂H₂[−] in variant H₃O⁺/NH₄⁺ concentration. The weakest bond strength in the ring of each naked heterocyclic anion is marked by a dashed line for comparison.

Compared with naked N₅[−], N₄C₁H₁[−], and N₃C₂H₂[−], the bonds of heterocycles in H₃O⁺/NH₄⁺ solvents were significantly enhanced, and this enhancement increased with the increase in H₃O⁺/NH₄⁺ concentration. For example, the weakest bond in the N₅[−] ··· 4H₃O⁺ complex was 145.24 kcal/mol, which was improved by 54% than that of the naked N₅[−]; the weakest bond in N₅[−] ··· 4NH₄⁺ was 140.54 kcal/mol and was improved by 48.7%. Similarly, the weakest bonds in the N₄C₁H₁[−] ··· 4H₃O⁺ and N₄C₁H₁[−] ··· 4NH₄⁺ were enhanced by 67% and 51%, respectively, compared with that of the naked N₄C₁H₁[−]; the weakest bonds in N₃C₂H₂[−] ··· 3H₃O⁺ and N₃C₂H₂[−] ··· 3NH₄⁺ were enhanced by 44% and 37%, respectively, compared with the naked N₃C₂H₂[−]. In contrast, the presence of benzene and THF surrounding N₅[−], N₄C₁H₁[−], and N₃C₂H₂[−] showed little influence on the strength of the bonds in the rings. Their influence on the weakest bond strength was in the range of −4.0–6.6%. Therefore, the H₃O⁺/NH₄⁺ ions showed a significant stabilization effect on the enhancement of the studied heterocyclic structures, in particular at a high concentration of H₃O⁺/NH₄⁺, implying a potential catalytic effect of the H₃O⁺/NH₄⁺ ions in the preparation of heterocyclic compounds.

The stabilization effect of the H₃O⁺/NH₄⁺ ions on the heterocyclic structures was caused by their HB interactions with the NLPE. Such HB interactions stretched the NLPE away from its original position, thereby reducing the inter-lone-pair repulsion within the σ -aromatic system. In contrast, since the HB interactions between the heterocycles and the benzene/THF were very weak, the location of the NLPE in the heterocycles was almost unaffected. Therefore, the two solvents showed little effect on the structural stability of the heterocycles.

3. Methodology

The heterocyclic anions studied here include the pentazole anion N_5^- , tetrazole anion $N_4C_1H_1^-$, and 1,2,4-triazole anion $N_3C_2H_2^-$. In order to evaluate the influence of the acidity and concentration of the solvent on the reactivity of heterocyclic anions, we built atomistic models for each heterocyclic anion by traversing the four solvents of H_3O^+ , NH_4^+ , benzene, and THF. For each type of solvent, the molar ratio of solvent to heterocyclic anion increased from $c = 1$ to $c = 5$. In addition, one naked anion laid in a vacuum was calculated for comparison. Therefore, 63 atomistic models were used for calculation and evaluation in total.

All the calculations were performed using a quantum mechanical method based on the density functional theory (DFT). The quantities of electron density, atomistic structure, interatomic interactions, MO, magnetic shielding, and energetics were calculated based on the corresponding optimized structure, which was obtained using Gaussian 09 at the B3LYP/6-31G(d) level [43]. After the optimization of the 63 atomistic models, 55 presented with clustered structures, with 1 heterocyclic anion present in the middle and solvent species distributed nearby, as shown in Figures S1–S3 of the Supplementary Materials. For the other 8 models with $c = [H_3O^+ \text{ or } NH_4^+]/[N_5^-, N_4C_1H_1^-, \text{ or } N_3C_2H_2^-] = 5$ and $c = [H_3O^+ \text{ or } NH_4^+]/[N_3C_2H_2^-] = 4$, the H_3O^+/NH_4^+ ions diffused away from the vicinity of the heterocyclic anions.

The strengths of the relevant interatomic interactions, including bonding interactions, nonbonding interactions, and antibonding interactions, were evaluated by the integrated value of the crystal orbital Hamilton population (COHP) below the Fermi energy, using a recently developed High Accuracy Atomistic Simulation for Energetic Materials (HASEM) package [44,45]. The number of electrons shared between atoms was characterized by the delocalization index (DI); a higher DI value suggests a stronger delocalization of the NLPE [46]. The aromaticity was quantified by NICS_{zz}, namely nucleus-independent chemical shifts, along the z-direction [47]. A considerable negative NICS_{zz} value indicates the presence of aromaticity, and this method is by far one of the most widely used magnetic shielding indexes for diagnosing aromaticity. All DI and NICS values were calculated at the B3LYP/6-311++G(d, p) level. We further separated DI and NICS into individual components contributed solely by π -electrons/lone-pair electrons, using the natural bond orbital (NBO) [48–50] analysis and the quantum theory of atoms in molecules (QTAIM) [51,52] method that was implemented in the Multiwfn application [53]. The indices with π/σ subscripts are the components contributed by all the π -electrons/ σ -electrons, whereas those with min- π /min- σ (LP) subscripts are the components contributed by the π -electrons/lone-pair σ -electrons at each lowest energy level.

The basicity of the nitrogen heterocyclic anions and the acidity of the solvents studied were evaluated by their proton affinity (PA) [54,55]:

$$PA = E_{\text{protonated}} - E_{\text{unprotonated}} \quad (1)$$

where $E_{\text{protonated}}$ is the total energy of the protonated species and $E_{\text{unprotonated}}$ is the total energy of the corresponding unprotonated species. The higher the PA, the stronger the base and the weaker the conjugate acid in the gas phase. Therefore, the heterocyclic anion with a higher PA is more basic, and the solvent with a lower PA is more acidic.

The energetics of the heterocyclic anion–solvent complexes were characterized by binding energy (BE):

$$BE = E_{\text{anion}} + \sum_1^c E_{\text{solvent}} - E_{\text{complex}} \quad (2)$$

where E_{anion} is the total energy of the naked heterocyclic anion, E_{solvent} is the total energy of a separate solvent ion or molecule, and E_{complex} is the total energy of the overall complex. A higher positive BE value implies that the interspecies interactions are more favorable and the complex is energetically more stable. Otherwise, the negative BE value indicates that the structure of the proposed complex is thermodynamically unstable.

4. Conclusions

We performed a series of quantum mechanical calculations to explore the stability and reactivity of the pentazole anion N_5^- , tetrazole anion $N_4C_1H_1^-$, and 1,2,4-triazole anion $N_3C_2H_2^-$ in four types of solvents with different acidities and concentrations. The main conclusions are as follows:

- (1) Through the analysis of electron density, atomistic structure, interatomic interactions, molecular orbital, magnetic shielding, and energetics, we confirmed the basicity of N_5^- , $N_4C_1H_1^-$, and $N_3C_2H_2^-$, and the presence of dual aromaticity in the three heterocyclic anions;
- (2) The three heterocyclic anions were found to violate the acid–base neutralization rule when confronting more than three H_3O^+/NH_4^+ ions. The mechanism of the anomalous reactivity of heterocyclic anions was found to be a competition between their basicity and dual aromaticity;
- (3) Due to the stretching effect of hydrogen bonding on the nitrogen lone-pair electrons, the H_3O^+/NH_4^+ ions showed a significant stabilization effect on the studied heterocyclic structures, in particular at a high concentration of H_3O^+/NH_4^+ . In contrast, benzene and THF presented little influence on the structural stability of heterocyclic anions.

Supplementary Materials: The following are available online at <https://www.mdpi.com/article/10.3390/catal11070766/s1>.

Author Contributions: Conceptualization and methodology, L.Z.; formal analysis, C.L.; writing—original draft preparation, C.L. and L.Z.; writing—review and editing, Y.H. and C.Q.S. All authors have read and agreed to the published version of the manuscript.

Funding: This research was funded by National Natural Science Foundation of China, grant number 12072045.

Data Availability Statement: Data is contained within the article or Supplementary Materials.

Acknowledgments: L.Z. would like to thank J.G. Zhang and L. Li for their helpful discussions.

Conflicts of Interest: The authors declare no conflict of interest.

References and Note

1. Klapötke, T.M. *Chemistry of High-Energy Materials*, 5th ed.; De Gruyter: Berlin, Germany, 2017.
2. Politzer, P.; Murray, J.S. (Eds.) *Energetic Materials Part 1. Decomposition, Crystal, and Molecular Properties*; Elsevier: Amsterdam, The Netherlands, 2003.
3. Shukla, M.K.; Boddu, V.M.; Steevens, J.A.; Damavarapu, R.; Leszczynski, J. *Energetic Materials: From Cradle to Grave*; Springer International Publishing: Cham, Switzerland, 2017; Volume 25.
4. Zhang, C.; Xue, X.; Cao, Y.; Zhou, J.; Zhang, A.; Li, H.; Zhou, Y.; Xu, R.; Gao, T. Toward low-sensitive and high-energetic co-crystal II: Structural, electronic and energetic features of CL-20 polymorphs and the observed CL-20-based energetic–energetic co-crystals. *CrystEngComm* **2014**, *16*, 5905–5916. [[CrossRef](#)]
5. Yu, Q.; Yang, H.; Imler, G.H.; Parrish, D.A.; Cheng, G.; Shreeve, J.N.M. Derivatives of 3,6-Bis(3-aminofurazan-4-ylamino)-1,2,4,5-tetrazine: Excellent energetic properties with lower sensitivities. *ACS Appl. Mater. Interfaces* **2020**, *12*, 31522–31531. [[CrossRef](#)]
6. Tang, Y.; Huang, W.; Imler, G.H.; Parrish, D.A.; Shreeve, J.N.M. Enforced planar FOX-7-like molecules: A strategy for thermally stable and insensitive π -conjugated energetic materials. *J. Am. Chem. Soc.* **2020**, *142*, 7153–7160. [[CrossRef](#)]
7. Zhong, K.; Xiong, Y.; Liu, J.; Zhang, C. Enhanced shockwave-absorption ability of the molecular disorder rooting for the reactivity elevation of energetic materials. *Energ. Mater. Front.* **2020**, *1*, 103–116. [[CrossRef](#)]
8. Sabin, J.R. *Advances in Quantum Chemistry*; Academic Press: Cambridge, MA, USA, 2014.
9. Jiao, F.; Xiong, Y.; Li, H.; Zhang, C. Alleviating the energy & safety contradiction to construct new low sensitivity and highly energetic materials through crystal engineering. *CrystEngComm* **2018**, *20*, 1757–1768.
10. Lee, K.-Y.; Chapman, L.B.; Cobura, M.D. 3-Nitro-1,2,4-triazol-5-one, a less sensitive explosive. *J. Energ. Mater.* **1987**, *5*, 27–33. [[CrossRef](#)]
11. Trzciński, W.A.; Szymańczyk, L. Detonation properties of low-sensitivity NTO-based explosives. *J. Energ. Mater.* **2005**, *23*, 151–168. [[CrossRef](#)]
12. Klapötke, T.M.; Sabaté, C.M. Bistetrazoles: Nitrogen-rich, high-performing, insensitive energetic compounds. *Chem. Mater.* **2008**, *20*, 3629–3637. [[CrossRef](#)]

13. Bölter, M.F.; Klapötke, T.M.; Kustermann, T.; Lenz, T.; Stierstorfer, J. Improving the energetic properties of dinitropyrazoles by utilization of current concepts. *Eur. J. Inorg. Chem.* **2018**, *2018*, 4125–4132. [[CrossRef](#)]
14. Dippold, A.A.; Izsák, D.; Klapötke, T.M. A Study of 5-(1,2,4-Triazol-C-yl)tetrazol-1-ols: Combining the benefits of different heterocycles for the design of energetic materials. *Chem. Eur. J.* **2013**, *19*, 12042–12051. [[CrossRef](#)] [[PubMed](#)]
15. Dippold, A.A.; Klapötke, T.M. Synthesis and characterization of 5-(1,2,4-Triazol-3-yl)tetrazoles with various energetic functionalities. *Chem. Asian J.* **2013**, *8*, 1463–1471. [[CrossRef](#)]
16. Steinhäuser, G.; Klapötke, T.M. “Green” pyrotechnics: A chemists’ challenge. *Angew. Chem. Int. Ed.* **2008**, *47*, 3330–3347. [[CrossRef](#)] [[PubMed](#)]
17. Huynh, M.H.V.; Hiskey, M.A.; Meyer, T.J.; Wetzler, M. Green primaries: Environmentally friendly energetic complexes. *Proc. Natl. Acad. Sci. USA* **2006**, *103*, 5409–5412. [[CrossRef](#)]
18. Chen, J.; Tang, J.; Xiong, H.; Yang, H.; Cheng, G. Combining triazole and furazan frameworks via methylene bridges for new insensitive energetic materials. *Energ. Mater. Front.* **2020**, *1*, 34–39. [[CrossRef](#)]
19. Liao, S.; Zhou, Z.; Wang, K.; Jin, Y.; Luo, J.; Liu, T. Synthesis of 5/6/5-fused tricyclic-cation-based cyclo-N₅[−] salt with high density and heat of formation. *Energ. Mater. Front.* **2020**, *3*, 172–177. [[CrossRef](#)]
20. Chen, S.; Jin, Y.; Xia, H.; Wang, K.; Liu, Y.; Zhang, Q. Synthesis of fused tetrazolo[1,5-b]pyridazine-based energetic compounds. *Energ. Mater. Front.* **2020**, *1*, 16–25. [[CrossRef](#)]
21. Glukhovtsev, M.N.; Dransfeld, A.; Schleyer, P.v.R. Why pentaphosphole, P₅H, is planar in contrast to phosphole, (CH)₄PH. *J. Phys. Chem.* **1996**, *100*, 13447–13454. [[CrossRef](#)]
22. Clayden, J.; Greeves, N.; Warren, S. *Organic Chemistry*, 2nd ed.; Oxford University Press: Oxford, UK, 2000.
23. Vegard, L. Crystal structure of solid nitrogen. *Nature* **1929**, *124*, 337. [[CrossRef](#)]
24. Patai, S. *The Chemistry of the Hydrazo, Azo and Azoxy Groups*; Wiley: New York, NY, USA, 1977; Volume 2.
25. Gray, P. *Chemistry and Physics of Energetic Materials*; Springer: Dordrecht, The Netherlands, 1990.
26. Nguyen, M.T. Polynitrogen compounds: 1. Structure and stability of N₄ and N₅ systems. *Coord. Chem. Rev.* **2003**, *244*, 93–113. [[CrossRef](#)]
27. Velian, A.; Cummins, C.C. Synthesis and characterization of P₂N₃[−]: An aromatic ion composed of phosphorus and nitrogen. *Science* **2015**, *348*, 1001–1004. [[CrossRef](#)] [[PubMed](#)]
28. Jiang, C.; Zhang, L.; Sun, C.; Zhang, C.; Yang, C.; Chen, J.; Hu, B. Response to comment on “Synthesis and characterization of the pentazolate anion cyclo-N₅[−] in (N₅)₆(H₃O)₃(NH₄)₄Cl”. *Science* **2018**, *359*, eaas8953. [[CrossRef](#)] [[PubMed](#)]
29. Huang, R.-Y.; Xu, H. Comment on “Synthesis and characterization of the pentazolate anion cyclo-N₅[−] in (N₅)₆(H₃O)₃(NH₄)₄Cl”. *Science* **2018**, *359*, eaao3672. [[CrossRef](#)]
30. Nguyen, M.T.; McGinn, M.A.; Hegarty, A.F.; Elguéro, J. Can the pentazole anion (N₅[−]) be isolated and/or trapped in metal complexes? *Polyhedron* **1985**, *4*, 1721–1726. [[CrossRef](#)]
31. Glukhovtsev, M.N.; Jiao, H.; Schleyer, P.v.R. Besides N₂, What is the most stable molecule composed only of nitrogen atoms? *Inorg. Chem.* **1996**, *35*, 7124–7133. [[CrossRef](#)]
32. Najafpour, J.; Foroutan-Nejad, C.; Shafiee, G.H.; Peykani, M.K. How does electron delocalization affect the electronic energy? A survey of neutral poly-nitrogen clusters. *Comput. Theor. Chem.* **2011**, *974*, 86–91. [[CrossRef](#)]
33. Zhang, L.; Yao, C.; Yu, Y.; Wang, X.; Sun, C.Q.; Chen, J. Mechanism and functionality of pnictogen dual aromaticity in pentazolate crystals. *ChemPhysChem* **2019**, *20*, 2525–2530. [[CrossRef](#)]
34. Zhang, L.; Yao, C.; Yu, Y.; Jiang, S.-L.; Sun, C.Q.; Chen, J. Stabilization of the dual-aromatic cyclo-N₅[−] anion by acidic entrapment. *J. Phys. Chem. Lett.* **2019**, *10*, 2378–2385. [[CrossRef](#)]
35. Zong, H.-H.; Yao, C.; Sun, C.Q.; Zhang, J.-G.; Zhang, L. Structure and stability of aromatic nitrogen heterocycles used in the field of energetic materials. *Molecules* **2020**, *25*, 3232. [[CrossRef](#)]
36. Li, Z.-H.; Moran, D.; Fan, K.-N.; Schleyer, P.v.R. σ -Aromaticity and σ -antiaromaticity in saturated inorganic rings. *J. Phys. Chem. A* **2005**, *109*, 3711–3716. [[CrossRef](#)] [[PubMed](#)]
37. Note: Current values of aromaticity indices of pentazole anion have slight difference from our previous publication on Stabilization of the Dual-Aromatic cyclo-N₅[−] Anion by Acidic Entrapment. *J. Phys. Chem. Lett.* **2019**, *10*, 2378, because of the use of a different optimization method. The NICS_{zz}(1)_{sigma} value for benzene is corrected to be −0.113.
38. Satchell, J.F.; Smith, B.J. Calculation of aqueous dissociation constants of 1,2,4-triazole and tetrazole: A comparison of solvation models. *Phys. Chem. Chem. Phys.* **2002**, *4*, 4314–4318. [[CrossRef](#)]
39. Lindstrom, P.; Mallard, W. *NIST Chemistry WebBook*; NIST Standard Reference Database Number 69; National Institute of Standards and Technology: Gaithersburg, MD, USA, 2003.
40. EP Serjeant, B.D. *Ionization Constants of Organic Acids in Solution*; Pergamon Press: Oxford, UK; New York, NY, USA, 1979.
41. Zhang, Z.; Li, D.; Jiang, W.; Wang, Z. The electron density delocalization of hydrogen bond systems. *Adv. Phys. X* **2018**, *3*, 1428915. [[CrossRef](#)]
42. Zhang, C.; Sun, C.; Hu, B.; Yu, C.; Lu, M. Synthesis and characterization of the pentazolate anion cyclo-N₅[−] in (N₅)₆(H₃O)₃(NH₄)₄Cl. *Science* **2017**, *355*, 374–376. [[CrossRef](#)]
43. Frisch, M.J.; Trucks, G.W.; Schlegel, H.B.; Scuseria, G.E.; Robb, M.A.; Cheeseman, J.R.; Scalmani, G.; Barone, V.; Mennucci, B.; Petersson, G.A.; et al. *Gaussian 09*; Gaussian: Wallingford, CT, USA, 2013.

44. Zhang, L.; Jiang, S.-L.; Yu, Y.; Long, Y.; Zhao, H.-Y.; Peng, L.-J.; Chen, J. Phase transition in octahydro-1,3,5,7-tetranitro-1,3,5,7-tetrazocine (HMX) under static compression: An application of the first-principles method specialized for CHNO solid explosives. *J. Phys. Chem. B* **2016**, *120*, 11510–11522. [[CrossRef](#)] [[PubMed](#)]
45. Mo, Z.; Zhang, A.; Cao, X.; Liu, Q.; Xu, X.; An, H.; Pei, W.; Zhu, S. JASMIN: A parallel software infrastructure for scientific computing. *Front. Comput. Sci. China* **2010**, *4*, 480–488. [[CrossRef](#)]
46. Poater, J.; Fradera, X.; Duran, M.; Solà, M. The delocalization index as an electronic aromaticity criterion: Application to a series of planar polycyclic aromatic hydrocarbons. *Chem. Eur. J.* **2003**, *9*, 400–406. [[CrossRef](#)]
47. Schleyer, P.v.R. Introduction: Aromaticity. *Chem. Rev.* **2001**, *101*, 1115–1118. [[CrossRef](#)] [[PubMed](#)]
48. Reed, A.E.; Curtiss, L.A.; Weinhold, F. Intermolecular interactions from a natural bond orbital, donor-acceptor viewpoint. *Chem. Rev.* **1988**, *88*, 899–926. [[CrossRef](#)]
49. Almeida, M.O.; Faria, S.H.D. Computational study of the alkylation reaction of the nitrogen mustard mechlorethamine using NBO model and the QTAIM theory. *Open J. Phys. Chem.* **2013**, *3*, 127–137. [[CrossRef](#)]
50. Reed, A.E.; Weinhold, F. Natural bond orbital analysis of near-Hartree–Fock water dimer. *J. Chem. Phys.* **1983**, *78*, 4066–4073. [[CrossRef](#)]
51. Bader R F, W. *Atoms in Molecules: A Quantum Theory, International Series of Monographs on Chemistry*; Clarendon Press: Oxford, UK, 1990.
52. Bader, R.F. Atoms in molecules. *Acc. Chem. Res.* **1985**, *18*, 9–15. [[CrossRef](#)]
53. Lu, T.; Chen, F. Multiwfn: A multifunctional wavefunction analyzer. *J. Comput. Chem.* **2012**, *33*, 580–592. [[CrossRef](#)] [[PubMed](#)]
54. Matijssen, C.; Kinsella, G.K.; Watson, G.W.; Rozas, I. Computational study of the proton affinity and basicity of structurally diverse α 1-adrenoceptor ligands. *J. Phys. Org. Chem.* **2012**, *25*, 351–360. [[CrossRef](#)]
55. Camaioni, D.M.; Schwerdtfeger, C.A. Comment on “Accurate experimental values for the free energies of hydration of H^+ , OH^- , and H_3O^+ ”. *J. Phys. Chem. A* **2005**, *109*, 10795–10797. [[CrossRef](#)] [[PubMed](#)]